

Remote preparation of arbitrary time-encoded single-photon ebits

Alessandro Zavatta,¹ Milena D'Angelo,² Valentina Parigi,³ and Marco Bellini^{1,2,*}

¹*Istituto Nazionale di Ottica Applicata - CNR, L.go E. Fermi, 6, I-50125, Florence, Italy*

²*LENS, Via Nello Carrara 1, 50019 Sesto Fiorentino, Florence, Italy*

³*Department of Physics, University of Florence, I-50019 Sesto Fiorentino, Florence, Italy*

(Dated: August 9, 2018)

We propose and experimentally verify a novel method for the remote preparation of entangled bits (ebits) made of a single-photon coherently delocalized in two well-separated temporal modes. The proposed scheme represents a remotely tunable source for tailoring arbitrary ebits, whether maximally or non-maximally entangled, which is highly desirable for applications in quantum information technology. The remotely prepared ebit is studied by performing homodyne tomography with an ultra-fast balanced homodyne detection scheme recently developed in our laboratory.

PACS numbers: 03.67.Mn, 42.50.Dv, 03.65.Wj

Entanglement, nonlocal correlations, indistinguishable alternatives are, historically, among the most intriguing and appealing topics of quantum mechanics. Besides their relevance in fundamental physics [1], these phenomena have attracted much attention due to their usefulness in quantum information technology [2]. Extravagant but promising protocols such as quantum teleportation, quantum cryptography, and quantum computation have been proposed and experimentally verified (see, e.g., [2] and references therein). All these schemes were originally based on two-photon entanglement. Recently, increasing attention has been given to a new quantum information perspective: the carriers of quantum information are no longer the photons, but rather the field modes “carrying” them. Based on this idea, two different approaches have been followed. The first one exploits the entanglement in momentum generated when a single-photon impinges on a beam-splitter and is characterized by the state $\alpha|1\rangle_a|0\rangle_b + \beta|0\rangle_a|1\rangle_b$, where a and b denote two distinct spatial modes, α and β are complex amplitudes such that $|\alpha|^2 + |\beta|^2 = 1$ (see, e.g., [3, 4] and references therein). The second and more recent road has been traced by Gisin’s group [5] on the line of Franson’s approach [6], and leads to two-photon systems entangled in ultra-short co-propagating temporal modes (or “time-bins”) [7].

In this Letter, we propose the first remotely tunable source of arbitrary single-photon entangled states (ebits) in the time domain and experimentally demonstrate its working principle. We start from the spontaneous parametric down conversion (SPDC) signal-idler pairs [8] generated by a train of phase-locked pump pulses [5, 9] and generate indistinguishability between pairs of consecutive non-overlapping temporal modes propagating in the idler channel; this enables us to remotely delocalize the twin signal photon between two identical and well-separated time-bins, thus generating the single-photon temporal ebit: $\alpha|1^{(n)}\rangle|0^{(n+1)}\rangle + \beta|0^{(n)}\rangle|1^{(n+1)}\rangle$, where n denotes

the temporal mode associated with the n^{th} pump pulse. Both maximally and non-maximally entangled single-photon states, with any relative phase, can be produced by performing simple and reversible operations in the remote idler channel. The proposed scheme may find immediate application in quantum information technology; single-photon ebits have been proven to enable linear optics quantum teleportation [3, 10] and play a central role in linear optics quantum computation [4, 11]. Furthermore, time-bin entanglement has been proven suitable for long distance applications [10, 12], where the insensitivity to both depolarization and polarization fluctuations becomes a strong requirement. In addition, since the carriers of entanglement are naturally separated (i.e., no further optical element is required) and undergo the same losses, entanglement in time is less sensitive to losses and easier to purify [13].

The experimental setup is pictured in Fig. 1. The 1.5 ps pulses at 786 nm from a mode-locked Ti:Sapphire laser at a repetition rate of 82 MHz are frequency doubled in a LBO crystal. The resulting pulse train impinges on a non-linear BBO crystal cut for degenerate ($\Omega_s = \Omega_i = \Omega_p/2$) non-collinear type-I SPDC; signal-idler photon pairs centered around 786 nm are thus generated in two distinct spatial modes. A single mode fiber and a pair of etalon interference filters (F) are employed for spatial and spectral filtering of the idler beam before its entrance in a fiber-coupled piezo-controlled (PZT) Michelson interferometer; a single-photon detector (D_1) is inserted at the exit port of the interferometer. The signal beam propagates in free space before being mixed at a 50-50 beam-splitter (BS) with a local oscillator (LO) for high-frequency time-domain balanced homodyne detection (HD) [14, 15]. Spatial and spectral filtering of the idler mode guarantees the conditional projection of the signal photons into a single-photon pure state [16, 17, 18]. On the other hand, the Michelson interferometer generates indistinguishability between two consecutive temporal modes propagating in the idler channel: an idler photon detected by D_1 may have been generated by either the N^{th} or the $(N+1)^{\text{th}}$ pump pulse, provided that the time delay (T) between the short and long arms of

*Electronic address: bellini@inoa.it

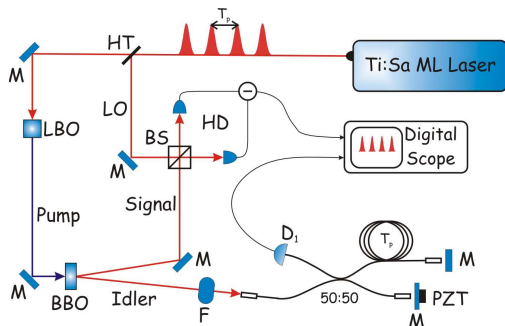


FIG. 1: (Color online) Schematic representation of the experimental setup. 50:50 is a 3 dB fiber coupler, HT a high-transmission beam splitter, and M are mirrors. See text for further details.

the interferometer is chosen to be approximately equal to the time separation between two consecutive pump pulses ($T_p = 12.3$ ns). Notice that the bandpass of the spectral filter in the idler arm ($\sigma_i = 50$ GHz) is wide enough so that no first order interference occurs ($\sigma_i \gg \pi/T_p$).

Based on a standard quantum mechanical calculation, we find that the combination of indistinguishability and tight filtering in the idler channel allows the conditional remote preparation, in the signal channel, of the temporally delocalized single-photon ebit:

$$|\Psi_s^{\phi_i}\rangle = \frac{1}{\sqrt{2}}(|1^{(n)}, 0^{(n+1)}\rangle + e^{-i\phi_i}|0^{(n)}, 1^{(n+1)}\rangle), \quad (1)$$

with $\phi_i = \Omega_p(T_p - T/2)$. Interestingly, the relative phase ϕ_i characterizing the remotely prepared ebit is defined not only by the phase difference introduced by the Michelson interferometer ($\varphi_{int} = \Omega_i T$), but also by the relative phase between consecutive pump pulses ($\varphi_{pump} = \Omega_p T_p$). The result of Eq. (1) represents the temporal counterpart of the spatially delocalized single-photon produced at the output ports of a beam splitter; this case has been studied experimentally by Babichev, *et al.* [19]. However, different from Ref. [19], the entangled state of Eq. (1) has been prepared remotely, without performing any manipulation on the signal photons. It is the interferometer in the idler arm which generates indistinguishability between two consecutive non-overlapping temporal modes; this indistinguishability, together with the coherence of both pump beam and SPDC process, gives rise, in the signal channel, to the coherent superposition of two previously independent and still temporally separated time-bins. An important advantage of such a remote state preparation scheme is the possibility of generating both maximally and non-maximally single-photon entangled states, with any relative phase ϕ_i , by performing simple and reversible operations in the idler arm (or on the train of pump pulses). For instance, two of the four Bell states, namely $|\Psi_s^{\pm}\rangle = \frac{1}{\sqrt{2}}(|1^{(n)}, 0^{(n+1)}\rangle \pm |0^{(n)}, 1^{(n+1)}\rangle)$, can be easily generated by manipulating the interferometer. Furthermore, the probability amplitudes characterizing the de-

localized single-photon may be continuously varied by simply introducing controllable losses in one arm of the interferometer; this has the only effect of lowering the production rate but does not introduce any impurity in the state generated in the signal channel.

The expected two-mode Wigner function [22] for the delocalized single-photon of Eq. (1) is given by:

$$W^{\phi_i}(x_1, y_1; x_2, y_2) = \frac{1}{2}[8W_{10}^{\phi_i}(x_1, y_1; x_2, y_2) + W_1(x_1, y_1)W_0(x_2, y_2) + W_0(x_1, y_1)W_1(x_2, y_2)], \quad (2)$$

where $W_1(x, y) = \frac{2}{\pi}e^{-2x^2}e^{-2y^2}(4x^2 + 4y^2 - 1)$ and $W_0(x, y) = \frac{2}{\pi}e^{-2x^2}e^{-2y^2}$ are the single-mode Wigner functions associated with a single-photon Fock state and with the vacuum, respectively; on the other hand, $W_{10}^{\phi_i}(x_1, y_1; x_2, y_2)$ is a non-factorable 4-D function which couples the quadratures of two consecutive non-overlapping signal temporal modes:

$$W_{10}^{\phi_i}(x_1, y_1; x_2, y_2) = W_0(x_1, y_1)W_0(x_2, y_2) \times (x_1 x_2^{\phi_i} + y_1 y_2^{\phi_i}), \quad (3)$$

where $x_2^{\phi_i} = x_2 \cos \phi_i - y_2 \sin \phi_i$ and $y_2^{\phi_i} = x_2 \sin \phi_i + y_2 \cos \phi_i$. Then, the Wigner function associated with the delocalized signal photon contains information about the characteristic phase ϕ_i introduced through the idler arm. Also notice that, by introducing the phase-dependent correlation quadratures $x_{\pm}^{\phi_i} = (x_1 \pm x_2^{\phi_i})/\sqrt{2}$, and $y_{\pm}^{\phi_i} = (y_1 \pm y_2^{\phi_i})/\sqrt{2}$, the Wigner function of Eq. (2) factors:

$$W(x_+^{\phi_i}, y_+^{\phi_i}; x_-^{\phi_i}, y_-^{\phi_i}) = W_1(x_+^{\phi_i}, y_+^{\phi_i}) \times W_0(x_-^{\phi_i}, y_-^{\phi_i}). \quad (4)$$

This result explicitly indicates that the delocalized single-photon cannot be described in terms of the quadratures associated with neither one of the two distant temporal modes (1 and 2), separately; however, the single-photon is well defined in the phase space $(x_+^{\phi_i}, y_+^{\phi_i})$, while the vacuum is defined in the phase space $(x_-^{\phi_i}, y_-^{\phi_i})$. Thus, the 4-D Wigner function reproduces the correlations remotely generated between pairs of well-separated temporal modes in the signal arm.

We have experimentally verified the correctness of the above predictions by performing balanced homodyne tomography and reconstructing both the density matrix and the Wigner function of the ebit remotely prepared in the signal channel. The density matrix has been reconstructed directly from the homodyne data by employing the method developed by D'Ariano, *et al.* [20]; its elements have then been used to reconstruct the Wigner function (for more details see our previous works [15, 21]).

In order to reconstruct the two-mode 4-D Wigner function of Eq. (2), one would normally need to measure the joint marginal distribution of the quadratures $X_1(\theta_1) = x_1 \cos \theta_1 - y_1 \sin \theta_1$ and $X_2(\theta_2) = x_2 \cos \theta_2 - y_2 \sin \theta_2$, while varying the phases θ_1 and θ_2 of two LO pulses spatially and temporally matched (i.e., synchronized) to the

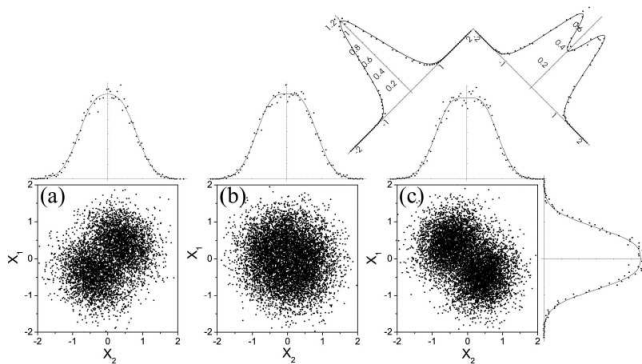


FIG. 2: Joint marginal distributions of the measured two-mode field quadratures for: (a) $\phi_i = -\Delta\theta$, (b) $\phi_i = \pi/2 - \Delta\theta$, (c) $\phi_i = \pi - \Delta\theta$, while leaving $\Delta\theta$ fixed. These are also the joint marginal distributions $p(X_1, X_2, \Delta\theta)$ associated with the ebit of Eq. (1) for $\phi_i = 0$, and corresponding, respectively, to $\Delta\theta = 0, \pi/2, \pi$. The histograms are the single-mode marginal distributions $p(X_1)$ and $p(X_2)$ together with the corresponding best fits. The marginals for the x_{\pm} quadratures are plotted on the diagonal axes above (c).

modes 1 and 2, respectively. However, the particular state investigated here is invariant with respect to the global phase, and only the relative phase $\Delta\theta = \theta_1 - \theta_2$ needs to be controlled in the experiment [19, 22]. Moreover, the joint marginal distribution is invariant under interchange of ϕ_i and $\Delta\theta$. We exploited this property in order to overcome the difficulty connected to the generation of a pair of phase-controllable LO pulses out of the train coming from the laser. Rather than varying the relative LO phase, one may keep $\Delta\theta$ fixed (by just using any two consecutive pulses directly from the mode-locked train) and vary the phase ϕ_i by means of the interferometer. Although what we actually do in this case is to measure fixed quadratures on the two modes for a varying quantum state $|\Psi_s^{\phi_i}\rangle$, it is immediate to show that this is equivalent to performing a conventional LO phase scan of the fixed quantum state $|\Psi_s^{\phi_i=const}\rangle$. We shall name this technique as “remote balanced homodyne tomography”.

For each value of the interferometer phase φ_{int} and upon detection of an idler photon, stable and fast quadrature measurements have been realized on the corresponding pair of consecutive signal time-bins (plus one containing just the vacuum and used for calibration), while keeping both the local oscillator and the homodyne detection apparatus unchanged. A total of 10^6 quadrature measurements, equally distributed over the range $[0, \pi]$ of φ_{int} , has been performed on each of the three time-bins. The experimental results are reported in Fig. 2, where we plot the measured values of the quadratures X_1 and X_2 obtained for three different values of the remote phase ϕ_i , while leaving $\Delta\theta$ fixed. According to the above reasoning, these results also represent the marginal distributions $p(X_1, X_2, \Delta\theta)$ associated with the ebit of

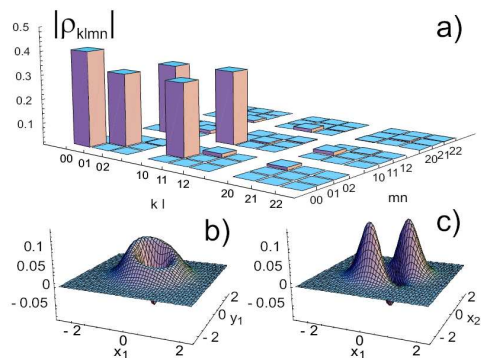


FIG. 3: (Color online) (a) Reconstructed density matrix elements $\rho_{klmn} = \langle k_1 l_2 | \hat{\rho} | m_1 n_2 \rangle$ corresponding to the state of Eq. (1) with $\phi_i = 0$. Cross sections of the reconstructed 4-D Wigner function: (b) $W^{\phi_i=0}(x_1, y_1; -0.1, -0.1)$, and (c) $W^{\phi_i=0}(x_1, 0; x_2, 0)$.

Eq. (1) for $\phi_i = 0$, and obtained for three different values of the relative phase $\Delta\theta$. Notice that, while the joint distribution $p(X_1, X_2, \Delta\theta)$ is strongly phase-dependent, the marginal distributions $p(X_1)$ and $p(X_2)$ associated with each temporal mode, separately, are phase-independent. This is consistent with the fact that each mode, separately, is an incoherent statistical mixture of vacuum and single-photon Fock state; however, the pair of modes 1 and 2, as a whole, is in the coherent superposition described by Eq. (1), with $\phi_i = 0$. Figure 2 also shows that a single-photon Fock state is defined in the phase space $(x_+^{\phi_i=0}, y_+^{\phi_i=0})$, while the vacuum is defined in the phase space $(x_-^{\phi_i=0}, y_-^{\phi_i=0})$, as expected from Eq. (4).

Figure 3 (a) reports the reconstructed density matrix: $\hat{\rho} = (1 - \eta)|0\rangle\langle 0| + \eta|\Psi_s^{\phi_i=0}\rangle\langle\Psi_s^{\phi_i=0}|$, where the overall efficiency $\eta = 60.5\%$ accounts for both preparation and detection efficiencies; notice that almost no multi-photon contribution exists. From this figure it is also apparent that the vacuum contamination, hence the losses, does not degrade the coherence of the remotely delocalized single-photon; in fact, both the non-diagonal and the diagonal ($|01\rangle\langle 01|$ and $|10\rangle\langle 10|$) elements of the reconstructed density matrix are reduced by the same amount. This may be understood as a consequence of the common losses undergone by the pair of entangled time-bins. Figures 3(b) and (c) reproduce, respectively, the (x_1, y_1) and (x_1, x_2) sections of the reconstructed 4-D Wigner function $W^{\phi_i=0}(x_1, y_1, x_2, y_2)$. The cross section (x_1, y_1) resembles the standard Wigner function of a single-photon Fock state, but is characterized by a well-defined phase; the existence of this phase is the result of the coherent delocalization of the single-photon between two separate temporal modes. The (x_1, x_2) section of the reconstructed Wigner function explicitly shows the correlation between the quadratures x_1 and x_2 ; the non-factorable nature of the delocalized single-photon is here apparent.

In summary, the experimental reconstruction of the

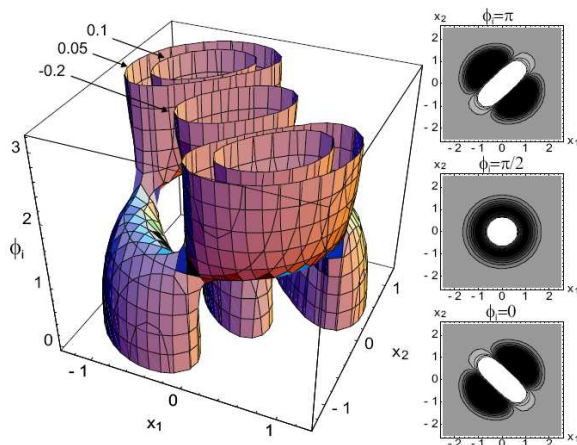


FIG. 4: (Color online) 3-D contour plot of the Wigner function section $W^{\phi_i}(x_1, 0, x_2, 0)$ associated with the single-photon ebit of Eq. (1) versus its characteristic remotely tunable phase ϕ_i . The surfaces shown correspond to three values of the Wigner function, namely: $W^{\phi_i} = -0.2, 0.05, 0.1$. Insets: contour plots for three specific values of the phase ϕ_i .

Wigner function of the conditionally prepared single-photon ebit has enabled us to verify its entangled nature and study its purity. Beside the non-classical behavior typical of single-photon Fock states (negative values around the origin), the reconstructed 4-D Wigner function has been found to be characterized by an intriguing phase information and by correlation between well separated temporal modes, as expected from Eq. (2). It may seem counterintuitive that a single photon simultaneously affects two non-overlapping temporal modes or, equivalently, carries a well defined phase. However, the effect is a direct consequence of the coherent superpo-

sition remotely induced between otherwise independent signal time-bins; it can then be understood in terms of quantum entanglement between two co-propagating but distinct temporal modes carrying a single-photon.

From the applicative viewpoint, one of the most interesting aspects of the proposed scheme is the dependence of the relative phase characterizing the delocalized (signal) single photon on both the relative phase between pump pulses and the phase delay introduced by the remote Michelson interferometer. Based on this effect, for any fixed value of the remotely controlled phase ϕ_i , one may generate, in the signal arm, a specific single-photon ebit. This point is pictorially demonstrated by Fig. 4, where we draw the contour plots of the (x_1, x_2) section of the 4-D Wigner function for all possible values of the remotely tunable phase ϕ_i characterizing the ebit of Eq. (1). The Wigner function $W^{\phi_i}(x_1, 0; x_2, 0)$ associated with each conditionally prepared ebit $|\Psi_s^{\phi_i}\rangle$ reveals a specific correlation between the field quadratures of two distinct signal temporal modes; as the preparation phase ϕ_i is changed from 0 to π , we observe the transition from correlated to anti-correlated quadratures through a “saddle” point at $\phi_i = \pi/2$, where the anti-correlation is transferred into the quadrature space (x_1, y_2) (not shown in figure). In other words, the proposed scheme can be regarded as a remotely tunable source of arbitrary single-photon ebits; such a source is highly desirable for applications in quantum information technology.

This work has been performed in the frame of the “Spettroscopia laser e ottica quantistica” project of the Physics Department of the University of Florence and partially supported by Ente Cassa di Risparmio di Firenze and MIUR, under the FIRB contract RBNE01KZ94. M.D. acknowledges the support of Marie Curie RTN.

-
- [1] A. Einstein, B. Podolsky, and N. Rosen, *Phys. Rev.* **47**, 777 (1935). J.S. Bell, *Physics* **1**, 195 (1964).
[2] C.H. Bennett, and B.D. DiVincenzo, *Nature* **404**, 247 (2000)
[3] S. Giacomini *et al.*, *Phys. Rev. A* **66**, 030302 (2002)
[4] E. Knill, R. Laflamme, and G.J. Milburn, *Nature (London)* **409**, 46 (2001)
[5] J. Brendel *et al.*, *Phys. Rev. Lett.* **82**, 2594 (1999); H. de Riedmatten *et al.*, *Phys. Rev. A* **69**, 050304 (2004)
[6] J.D. Franson, *Phys. Rev. Lett.* **62**, 2205 (1989)
[7] C. Simon, and J.-P. Poizat, *Phys. Rev. Lett.* **94**, 030502 (2005)
[8] D.N. Klyshko, *Photon and Nonlinear Optics*, Gordon and Breach Science, New York, 1988
[9] T.E. Keller, and M.H. Rubin, *Phys. Rev. A* **56**, 1534 (1997); Y.-H. Kim *et al.*, *Phys. Rev. A* **62**, 043820 (2000)
[10] H. de Riedmatten *et al.*, *Phys. Rev. Lett.* **92**, 047904 (2004)
[11] T. B. Pittman, B. C. Jacobs, and J. D. Franson, *Phys. Rev. A* **71**, 032307 (2005)
[12] W. Tittel, J. Brendel, H. Zbinden, and N. Gisin, *Phys. Rev. Lett.* **84**, 4737 (2000)
[13] I.L. Chuang, and Y. Yamamoto, *Phys. Rev. Lett.* **76**, 4281 (1996)
[14] A. Zavatta *et al.*, *J. Opt. Soc. Am. B* **19**, 1189 (2002)
[15] A. Zavatta, S. Viciani, and M. Bellini, *Phys. Rev. A* **70**, 053821 (2004)
[16] T. Aichele, A.I. Lvovsky, and S. Schiller, *Eur. Phys. J. D* **18**, 237 (2002)
[17] M. Bellini *et al.*, *Phys. Rev. Lett.* **90**, 043602 (2003)
[18] S. Viciani, A. Zavatta, and M. Bellini, *Phys. Rev. A* **69**, 053801 (2004)
[19] S.A. Babichev, J. Appel, and A.I. Lvovsky, *Phys. Rev. Lett.* **92**, 193601 (2004)
[20] G.M. D’Ariano, C. Macchiavello, and M.G.A. Paris, *Phys. Rev. A* **50**, 4298 (1994)
[21] A. Zavatta, S. Viciani, and M. Bellini, *Science* **306**, 660 (2004); and *Phys. Rev. A* **72**, 023820 (2005)
[22] U. Leonhardt, *Measuring the Quantum State of Light*, Cambridge University Press, Cambridge, 1997